# UTILITY OF TECTONIC CLASSIFICATION DIAGRAMS FOR METAMORPHOSED BASIC ROCKS: A CASE STUDY FROM A SUITE OF BASIC ROCKS FROM MAKROHAR AREA,MADHYA PRADESH

Name: Swagata Maity
Exam roll no: MGEO194012
Registration no: 128260 of 2014-15
Department of Geological Sciences.
Jadavpur University
2018-2019

## CERTIFICATE FROM THE SUPERVISOR

This is to certify that **Ms. Swagata Maity** has worked under the supervision of Prof. Pulak Sengupta in the Department of Geological Sciences, Jadavpur University and completed her thesis entitled **"Utility of tectonic classification diagrams for metamorphosed basic rocks: a case study from a suite of basic rocks from Makrohar area, Madhya Pradesh"** which is being submitted towards the partial fulfillment of her M.Sc. Final Examination in Applied Geology of Jadavpur University in 2019.

**Signature of the Supervisor:**

Prof. Pulak Sengupta
Dept. of Geological Sciences
Jadavpur University

Dr. Pulak Sengupta
Professor
Department of Geological Sciences
Jadavpur University, Kolkata-700032

**Signature of Head of the Department:**

30/05/2019

Prof. Sanjoy Sanyal
Dept. of Geological Sciences
Jadavpur University

Head
Department of Geological Sciences
Jadavpur University
Kolkata-700032

# CONTENTS

# ABSTRACT

The CITZ is an ensemble of several low to medium-grade supracrustal belts, gneisses, granitoids and a few linear tracts of granulite belts, all of which are intruded by a suite of mafic rocks. We focus on the metaigneous mafic rocks, which occur as dykes and lensoidal bodies that intruded the granitic country rocks. It has a sharp contact with the host felsic rocks, and usually appear fine grained massive rock. The mafic dyke is mainly Gabbro to Troctolite or olivine bearing Gabbro in composition. The rock has been variably altered and metamorphosed. Unaltered samples preserve the magmatic subophitic texture which suggests rock was formed due to rapid cooling at shallow crustal depth. Geochemical study of the rock suggests that Protolith magmas of the mafic dykes emplaced in the northern segment of the CITZ is mainly tholeiitic basalt. Some rock samples are plotted in calc-alkaline field, but this enrichment of alkali elements Na + K is an artefact of alteration during metamorphism of the dykes. This basalt is slightly enriched in LREE & shows flat HREE pattern which resembles the composition of continental arc or flood basalts. Zr depletion, high to moderate $TiO_2$ supports this tholeiitic basalt is generated due to higher degree of partial melting of asthenopheric mantle. By applying tectonic discrimination diagram, the less altered samples do not yield proper constrain for interpreting the tectonic settings. So, these discrimination diagrams can not be used in every cases for interpreting the tectonic settings. Therefore, these diagrams should be used with caution and with proper support from other geological observations.

# 1. INTRODUCTION:

The CITZ (Central Indian Tectonic Zone, Fig.1) is an ensemble of several low-medium-grade supracrustal rocks, gneisses (both felsic and mafic) and granitoids (with minor high grade rocks) , all of which are intruded by a suite of mafic rocks. A number of crustal scale shear zones define the boundaries of the supracrustal belts, and variably and inhomogeneously deform the different rock types. In this study, we focus on the metaigneous mafic rocks, which occur as dykes and lensoidal bodies that intruded the granitic country rocks.

It is well established that generation of mafic dyke swarms within continental crust and their subsequent deformation and/or metamorphism represent a change in tectonic milieu from an extensional setup, when the magmatic protoliths of the mafic dykes were emplaced to a compressional setting when the deformation and metamorphism of the mafic dykes occurred (Mukherjee et al. 2018). Several recent studies have demonstrated that mafic dykes may be used as event stratigraphic markers as they are emplaced during the interlude period between two orogenic phases, which would otherwise remain unnoticed had these events been not separated through the emplacement of mafic dykes (Mukherjee et al. 2018 and references therein).

In general, basic magmas are the products of partial melting of ultramafic rocks in the Earth's upper mantle (Farmer, 2003). However, basic igneous rocks demonstrate a wide variety of mineralogical and compositional features. Tectonic setting of magma generation, degree of partial melting, depth of melting are some of the factors that control the compositional features of the magmas.

Mafic rocks are usually generated in the following main tectonic settings:

1. Ocean Island arc
2. Intraplate or within plate
3. Mid ocean ridge
4. Subduction zones

On the basis of protolith compositions from which the basic magmas are sourced, degree of partial melting and depth at which melt is generated, basic magma is divided into the following fundamental types

a) Tholeiitic magma – high degree of partial melting, variable depth
b) Alkaline magma - low degree of partial melting, high depth.

Furthermore, the composition and mineralogy (and texture) of basic rocks are influenced by depth of emplacement/intrusion, and the differentiation processes operating during crystallization. Accordingly, on the basis of geochemical characteristics of major, trace and rare earth elements, mafic rocks may be subdivided into the following types:.

1. Within-plate basalts (WPB)

2. Island- arc tholeiites (IAT)

3. Island-arc basalts (IAB)

4. Mid-ocean ridge basalts (MORB)

5. Ocean island tholeiite (OIT)

6. Ocean island alkaline basalt (OIA)

There are a number of published tectonic discrimination diagrams that are widely used to classify the above. Based on these tectonic discrimination diagrams, tectonic settings are inferred and associated tectonic models are

proposed in large number publications. Although in many cases these inferences corroborate with other geological observations (i.e. associated rock types, magmatism or metamorphism), sometimes the diagrams yield ambiguous results. This suggests that these tectonic discrimination diagrams have certain limitations and as outlined by several workers (cf. Pearce 1984, Whalen 1987). There are several factors (viz. fractionation, alteration, and assimilation) that influence the relative abundance of trace elements. Specifically, in case of metamorphosed igneous rocks, the composition of the rocks may be variably modified during metamorphism, such that the original compositional characteristics may only be partially preserved. In that case, depending on the degree of alteration, it becomes difficult to use their compositional features to characterize their protolith magmas.

In this study, we describe a suite of basic igneous rocks that have been variably altered and metamorphosed. We describe their compositional features and discuss the applicability of the tectonic discrimination diagrams in case of such metamorphosed igneous rocks.

# 2. REGIONAL GEOLOGY:

The Precambrian crust of central India comprises two Archaean cratonic domains (ca. 3.5-2.5 Ga), namely the Bundelkhand Craton in the north and Bastar Craton in the south (Roy et al.,2002). They were accreted along a broad, ENE-WSW trending Proterozoic (ca. 2.5-1.0 Ga) Central Indian Tectonic Zone (CITZ) (Fig. 1). The CITZ, as defined by Radhakrishna (1989) and Acharyya and Roy (2000), contains low- to medium-grade supracrustal belts set in largely undifferentiated gneisses and granitoids. A few tracts of granulites are present as enclaves within the gneisses. Amongst the supracrustal belts, the northern Mahakoshal belt (ca. 2.4-1.8 Ga), central Betul and southern Sausar belt (ca. 1.5-1.0 Ga) are prominent, of which Mahakoshal and Sausar belts are well studied. Further, the CITZ is traversed by number of crustal scale ductile shear zones, which mark either the boundaries of the supracrustal belts or discrete terrains, namely, Son-Narmada shear system, Tan shear and Central Indian Shear (Jain et al., 1991).
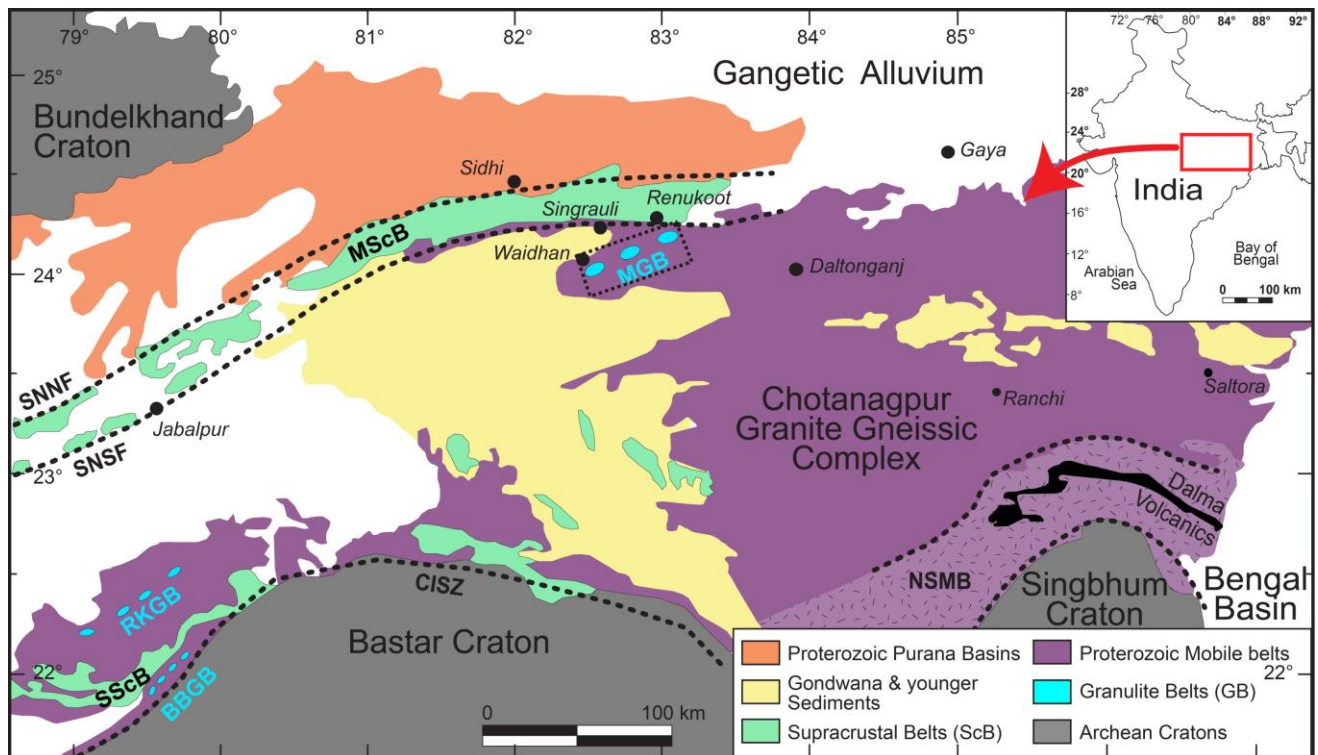
**Fig 1. Geological map showing different components of Eastern & Central India. BBGB- Balaghat–Bhandara Granulite Belt, CISZ—Central Indian Shear zone, MGB-Makrohar Granulite Belt, RKGB-Ramakona–Katangi Granulite Belt, SNNF-Sone Narmada North Fault,SNSF-Sone Narmada South Fault, NSMB-North Singbhum Mobile Belt. MSsB-Mahakoshal Supracrustal Belt. SScB-Sausar Supracrustal Belt.**

The southern segment of the CITZ is a complex collage of three litho-tectonic elements of contrasting thermal history: (a) The southern Bhandara-Balaghat granulite (BBG) domain, an association of podiform supracrustal and metaigneous granulites within granite gneisses records lower crustal ultra-high temperature granulite facies metamorphism along a counter clockwise (CCW) metamorphic P-T path (Bhowmik et al. 2005, 2014, Bhowmik, 2006, Bhowmik and Chakraborty, 2017). (b) The central domain of a stable platformal sequence of quartzite-pelite carbonate and Mn-oxide ore of the Sausar Group and its structurally underlying tonalite granodiorite-granite gneissic basement (type Tirodi biotite gneiss unit, Narayanaswami et al.1963; Pal and Bhowmik, 1998;

Bhowmik et al., 1999, 2011; Khan et al., 2002; Chattopadhyay et al., 2003a). The domain preserves a progressive Barrovian-type metamorphic sequence that shows north and northwestward increase in metamorphic grade from low greenschist to upper amphibolite facies (Narayanaswami et al., 1963; Pal and Bhowmik, 1998; Bhowmik et al., 2012). (c) The northern Ramakona-Katangi granulite (RKG) domain, a lithological association of granulites and charnockite that occur as rafts and lenses within the Tirodi biotite gneiss unit (Bhowmik and Roy 2003; Bhowmik and Spiering, 2004) shows high-pressure upper amphibolite to granulite facies metamorphism along a clockwise metamorphic P-T path (Bhowmik and Roy 2003; Bhowmik and Spiering, 2004).

Likewise, the northern segment of the CITZ is a juxtaposition of two litho-tectonic units. (a) The Makrohar granulite (MG) domain in the south, a lithological association of granulites and charnockites that occur as rafts and lenses within porphyritic granite gneisses. (b) The northern Mahakosal supracrustals comprising of a stable platformal sequence of quartzite-pelite carbonates metamorphosed under low P-high T conditions.

There are two broad types of metaigneous rocks: (a) a coarse-grained metagabbro norite (now two pyroxene granulite with or without garnet) to metanoritic composition that occurs as concordant sheet-like to lensoidal bodies within the supracrustal units. Geochemical studies reveal the gabbro-norite suite of tholeiitic composition was produced by 40% partial melting of variably enriched mantle sources and subsequent orthopyroxene clinopyroxene-plagioclase fractionation of parental melts (Alam et al., 2017). (b)The second variety of metaigneous rocks occurs as olivine gabbro and gabbro-norite dykes or lensoidal bodies that were emplaced within the gneissic country rocks and supracrustals (Fig. 2).

The present study focuses on the second variety of metaigneous rocks, from the northern segment of the CITZ.

**Fig 2.-Disposition of mafic dyke and the bands of calc-silicate rocks within felsic gneiss**.

The dykes have a sharp contact with the host felsic rocks, and usually appear fine grained massive (Fig. 3A). In rare cases, intergranular texturewith plagioclase laths are discernible in hand specimen (Fig. 3B)
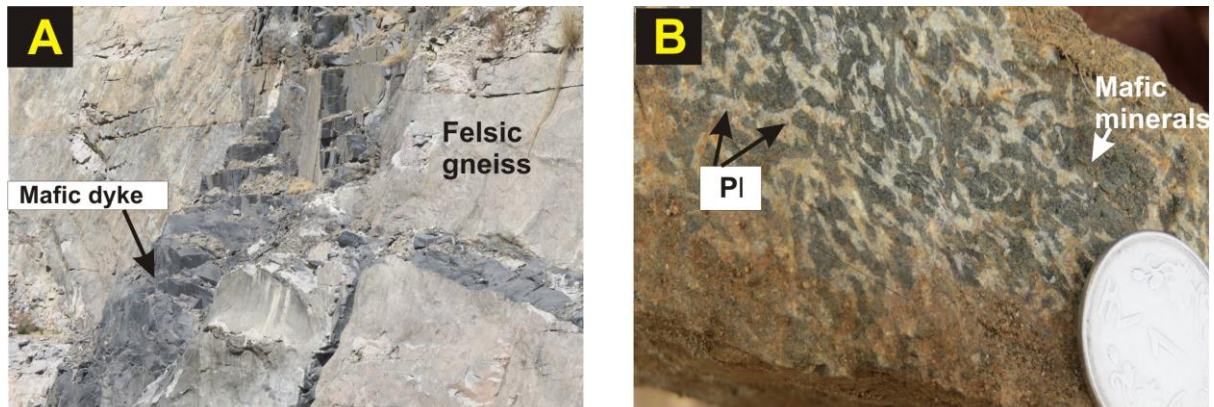
Fig.3. Field & Handspecimen photographs of mafic dyke. (A). Fine grained and massive mafic rock cuts across felsic gneiss.Contact between two is sharp. No chilled contact is present. (B). Intergranular to subophitic texture shown by plagioclase feldsper laths and mafic minerals (pyroxene and olivine) in some rock samples.

# 3. PETROGRAPHY:

Depending on the presence and modal abundance of primary (presumably magmatic) and secondary (metamorphic) minerals, and their textural relations, the samples have divided into 3 groups.

Group-1 (Least altered)

Group II (Moderately altered)

Group III (Intensely altered)

## Group-I

The samples (Sample no. SR-44(A), SR-46(D), SR-76(A), SR-76(B), SR-105(A), SR-116 & SR-147(A)) consist of mainly olivine, apatite, ilmenite, plagioclase feldspar, clinopyroxene as primary mineral, and orthopyroxene, amphibole, biotite as secondary minerals (<15-20 vol%). The primary minerals olivine, clinopyroxene and plagioclase dominantly show **subophitic intergranular** texture (Fig.4A). In some samples, plagioclase feldspar is fully covered by clinopyroxene grain defining **ophitic** texture (Fig.4B). Apatite and ilmenite occur in only one sample where apatite occurs as elongated cumulate needles that occur within an interstitial mass of ilmenite (Fig. 4C). Rarely, olivine also occurs as a cumulate phase with apatite (Fig. 4C). This association of Fe-Ti oxide, phosphate (FTP) , apatite and olivine occurs with plagioclase in the rock.

The secondary minerals occur as thin coronae around the primary ferromagnesian minerals, separating them from plagioclase: orthopyroxene and amphibole occur as spatially associated double coronae around olivine and ilmenite: orthopyroxene in contact with

olivine, and amphibole in contact with plagioclase (Fig.4D); biotite and amphibole occur as spatially associated double corona occur around ilmenite: biotite in contact with ilmenite, and amphibole in contact with plagioclase (Fig.4E); the biotite most likely replaces coronal orthopyroxene; orthopyroxene also replaces clinopyroxene (Fig. 4F).
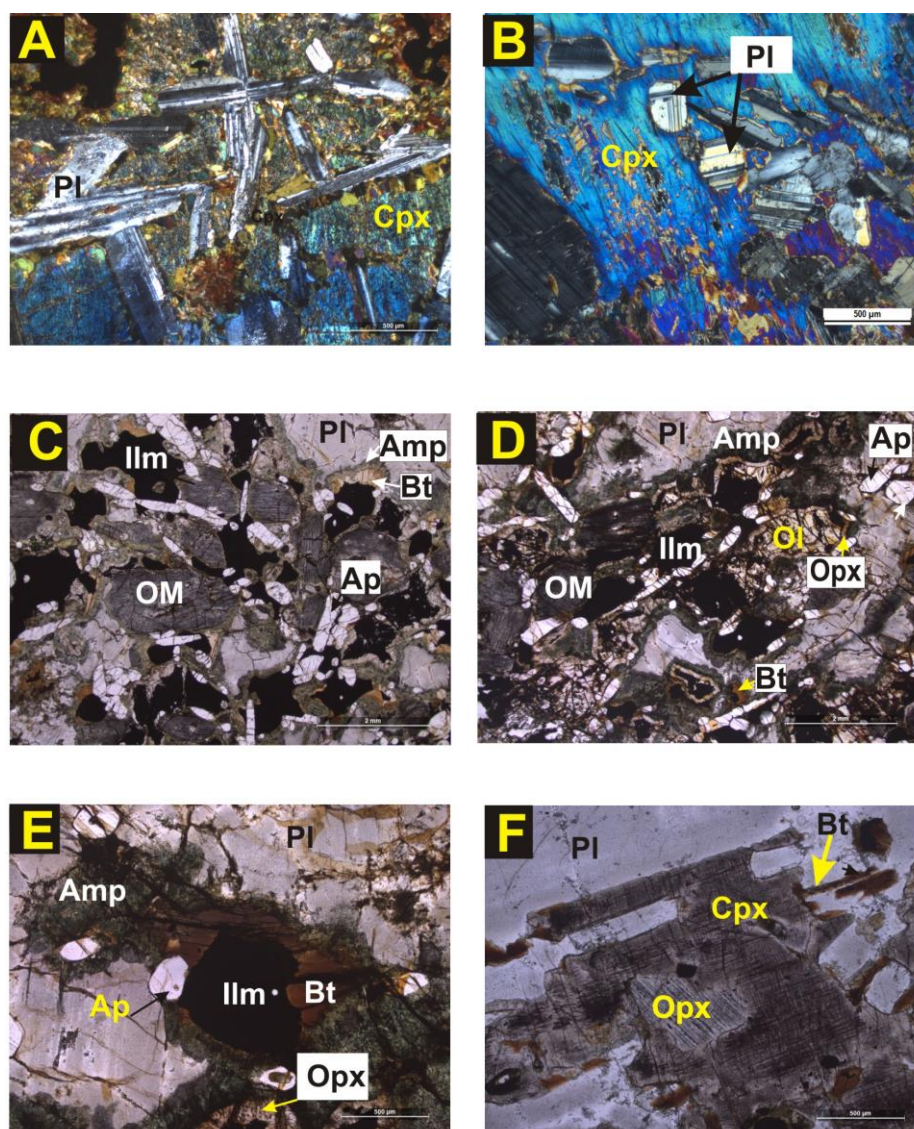
Fig 4. Photomicrograph shows textural features in the least altered samples(Group-I). (A)Subophitic -tntergranular Texture shown by plagioclase feldsper laths & clinopyroxene. (B). Plagioclase is included within cpx grain defining ophitic texture.(C-D). Cumulate texture defined by apatite needles & olivine grains and ilmenite is occuring in intercumulus spaces. (D).Double corona of orthopyroxene & amphibole separates ferromagnesium phases from plagioclase.Orthopyroxene corona occurs proximatly to ilmenite/olivine and amphibole corona occurs in contact with plagioclase. Ocationally biotite replaced orthopyroxene.(E).Ilmenite is surrounded by double corona of biotite (replacing orthopyroxene) & amphibole. (F). Secondary orthopyroxene replaced primary clinopyroxene.

# Group-II.

This group of samples (Sample no.-SR-41(A), SR-46(A-2), SR-63(F), SR-77, SR-82(B), SR-87(Z), SR-94(2), SR-103(A), SR-105(A),

SR-113 & SR-117) consist of mainly clinopyroxene, plagioclase feldspar and olivine as primary minerals and orthopyroxene, hornblende, biotite and muscovite as secondary minerals (~40-50 vol%). The replacement of the primary minerals by the secondary minerals occur in such a way that the general intergranular to subophitic texture is preserved (Fig. 5A-C). Olivine is either pseudomorphically replaced by a fine grained symplectite of orthopyroxene and magnetite (Fig. 5B), or by amphibole and magnetite (Fig. 5A). Ilmenite $\pm$ olivine is extensively replaced by biotite and amphibole (Fig. 5C). Clinopyroxene is altered to hornblende and biotite (Fig 5D). Some plagioclase feldspar grain shows the effects of sericitization (Fig.5E).
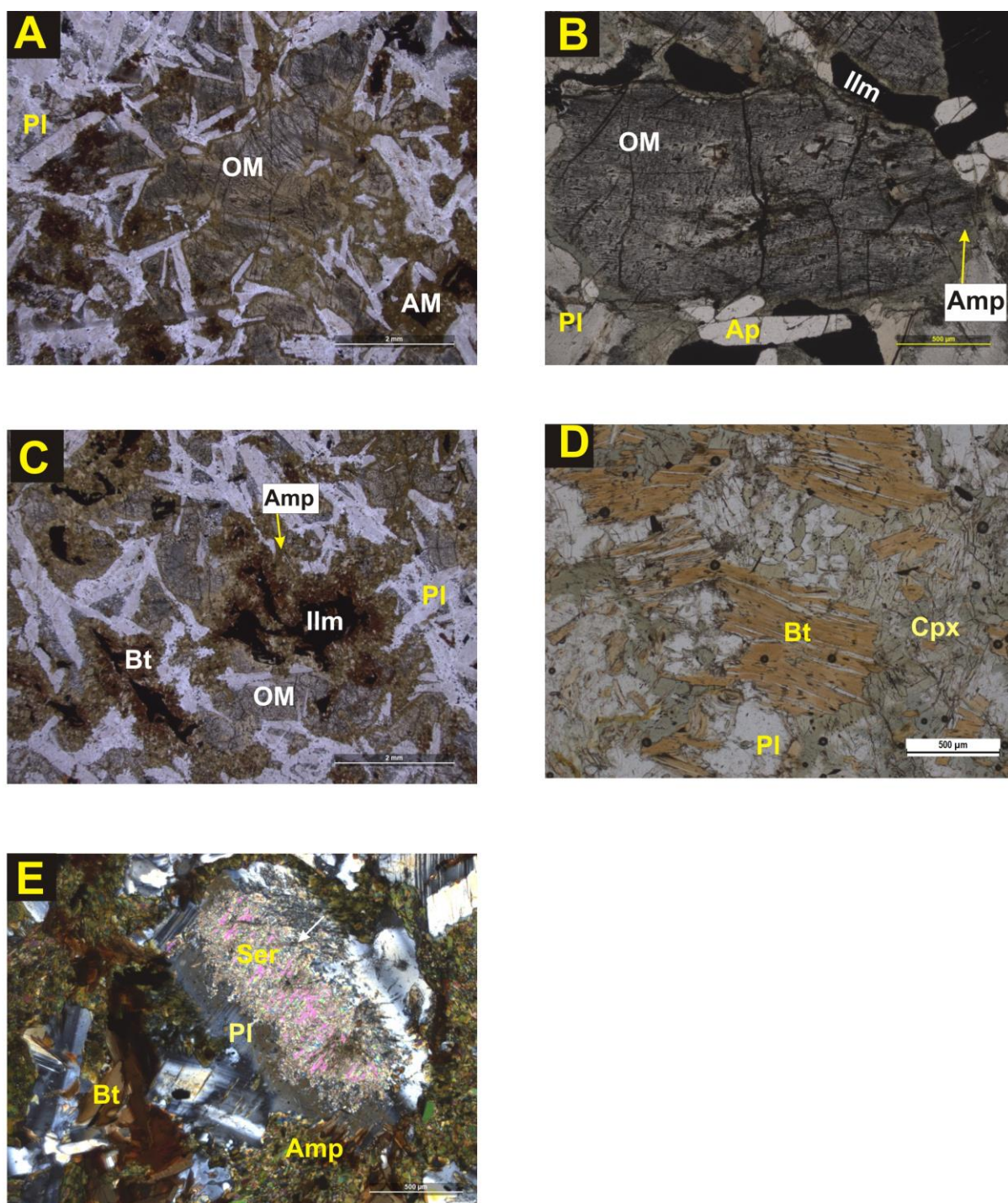
Fig 5. Photomicrograph showing textural features in the moderatly altered samples (Group-II) (A). Primary magmatic subophitic texture is preserved but primary magmatic olivine replaced by orthopyroxene & magnetite(OM) and clinopyroxene is replaced by amphibole and some magnetite (AM). (B). Fine grains of orthopyroxene & magnetite symplectite replaced olivine. (C). Primary magnetite subophitic texture preserved but only relict of primary ilmenite occurs within secondary biotite & amphibole.(D). Biotite replaced clinopyroxene. (E). Sericitization of plagioclase feldsper.

# Group-III

These samples (Sample no. SR-46(A-1), SR-46(B), SR-46(C), SR-48(A) & SR-87(Y)) primarily consists of plagioclase feldspar amphibole ± biotite (~90 vol%) whereas the primary minerals clinopyroxene and ilmenite occur as occasional relicts. Plagioclase and amphibole define a recrystallized granoblastic texture (Fig. 6). The grain size of the recrystallized mass varies from sample to sample.
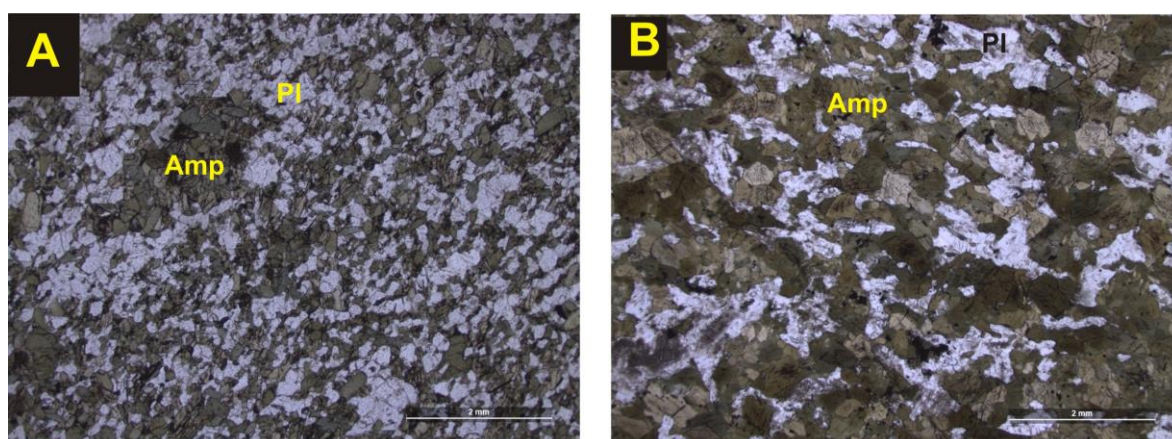


Fig 6.Photomicrograph shows textural features in the least altered sample (Group-III).(A-B). Recrystallized granoblastic texture defined by amphibole & plagioclase. Grainsize varies in 2 different sample(A & B).

# 4. NOMENCLATURE:

It is evident from the petrographic descriptions, that the primary magmatic mineralogy of the rock is plagioclase + olivine + clinopyroxene + FTP (in SR 76 only). However, the replacement of the primary minerals by a variety of secondary minerals makes it difficult to infer the mode of the primary minerals, and classify the rocks. Accordingly the CIPW norm is calculated (Cross et al, 1902, methodology outlined in Winter 2013, Table-1) from the whole rock major element data.

## Norm calculation for studied mafic dyke (Table-1)

| Sample No. | SR76B | SR76A | SR46E | SR46D | SR46A2 | SR46A1 | SR77 | SR44B |
|---|---|---|---|---|---|---|---|---|
| Quartz | 0 | 0 | 0.00 | 0.00 | 0.00 | 0.00 | 0.00 | 0.00 |
| Plagioclase | 52.59 | 49.82 | 54.25 | 51.20 | 51.06 | 70.60 | 65.04 | 31.88 |
| Orthoclase | 4.37 | 3.31 | 0.83 | 3.66 | 3.55 | 2.72 | 4.49 | 0.30 |
| Nepheline | 1.41 | 0.64 | 0.00 | 3.00 | 0.00 | 0.43 | 0.00 | 0.00 |
| Diopside | 6.69 | 5.81 | 19.38 | 7.70 | 9.21 | 10.47 | 6.49 | 1.05 |
| Hypersthene | 0 | 0 | 4.76 | 0.00 | 6.48 | 0.00 | 10.11 | 60.40 |
| Olivine | 21.22 | 24.4 | 18.78 | 21.94 | 27.00 | 13.78 | 13.09 | 2.41 |
| Ilmenite | 7.44 | 8.62 | 1.99 | 12.15 | 2.18 | 1.67 | 0.78 | 3.53 |
| Apatite | 6.33 | 7.46 | 0.07 | 0.39 | 0.56 | 0.37 | 0.09 | 0.44 |
| Chromite | 0 | 0 | 0.18 | 0.01 | 0.18 | 0.04 | 0.09 | 0.04 |
| Total | 100.5 | 100.6 | 100.24 | 100.05 | 100.22 | 100.08 | 100.18 | 100.05 |

| Sample No. | SR44A | SR41A | SR46B | SR46C | SR46F | SR63F | SR82B | SR87Z2 | SR94-2 |
|---|---|---|---|---|---|---|---|---|---|
| Quartz | 0.00 | 0.00 | 0.00 | 0.00 | 0.00 | 0.00 | 0.00 | 0.00 | 0.00 |
| Plagioclase | 31.86 | 40.47 | 49.99 | 66.44 | 65.61 | 44.43 | 42.24 | 42.71 | 44.48 |
| Orthoclase | 0.35 | 2.13 | 8.10 | 6.50 | 1.06 | 5.50 | 1.89 | 8.33 | 7.15 |
| Nepheline | 0.00 | 0.00 | 0.00 | 0.00 | 0.00 | 0.00 | 0.00 | 0.00 | 1.95 |
| Diopside | 1.28 | 31.57 | 16.30 | 9.86 | 4.98 | 16.79 | 29.19 | 17.67 | 16.78 |
| Hypersthene | 59.17 | 5.58 | 18.53 | 8.45 | 12.23 | 18.47 | 8.32 | 17.43 | 0.00 |
| Olivine | 3.39 | 17.36 | 4.13 | 5.76 | 15.07 | 13.35 | 15.88 | 10.44 | 23.61 |
| Ilmenite | 3.51 | 2.60 | 2.18 | 2.34 | 1.01 | 1.22 | 2.17 | 2.68 | 4.98 |
| Apatite | 0.44 | 0.30 | 0.76 | 0.65 | 0.07 | 0.23 | 0.30 | 0.74 | 1.07 |
| Chromite | 0.04 | 0.03 | 0.12 | 0.07 | 0.13 | 0.13 | 0.06 | 0.04 | 0.03 |
| Total | 100.04 | 100.04 | 100.11 | 100.07 | 100.16 | 100.13 | 100.05 | 100.05 | 100.06 |

| Sample No. | SR94-7 | SR103A | SR105A | SR113 | SR116 | SR117C | SR147 | SR87Y | SR87Z |
|---|---|---|---|---|---|---|---|---|---|
| Quartz | 0.00 | 0.00 | 0.00 | 0.00 | 0.00 | 1.18 | 9.60 | 7.61 | 0.00 |
| Plagioclase | 45.68 | 49.73 | 63.21 | 40.18 | 49.50 | 42.30 | 57.53 | 51.44 | 39.78 |
| Orthoclase | 7.45 | 10.64 | 1.30 | 6.56 | 1.95 | 9.93 | 2.54 | 13.53 | 11.52 |
| Nepheline | 1.15 | 0.00 | 0.00 | 0.00 | 0.00 | 0.00 | 0.00 | 0.00 | 0.00 |
| Diopside | 16.17 | 12.54 | 7.72 | 27.60 | 25.75 | 15.09 | 24.49 | 10.65 | 16.66 |
| Hypersthene | 0.00 | 11.28 | 1.57 | 7.35 | 5.34 | 29.43 | 4.79 | 13.79 | 21.15 |
| Olivine | 23.93 | 12.16 | 25.54 | 15.26 | 16.76 | 0.00 | 0.00 | 0.00 | 7.40 |
| Ilmenite | 4.60 | 2.85 | 0.55 | 2.72 | 0.53 | 1.65 | 0.84 | 2.18 | 2.70 |
| Apatite | 1.04 | 0.81 | 0.14 | 0.32 | 0.21 | 0.42 | 0.21 | 0.79 | 0.76 |
| Chromite | 0.03 | 0.01 | 0.01 | 0.03 | 0.03 | 0.04 | 0.06 | 0.01 | 0.03 |
| Total | 100.06 | 100.05 | 100.04 | 100.02 | 100.07 | 100.07 | 100.06 | 100.03 | 100.03 |

Thus, based on the normative abundance of the primary minerals (Fig. 7):

➢ The rock is plagioclase rich, i.e. anorthositic.

➢ Few samples plot within the **gabbro** field, few within the **troctolite** field, but most samples plot in between.

➢ Accordingly, the rock may be called an **olivine gabbro.**
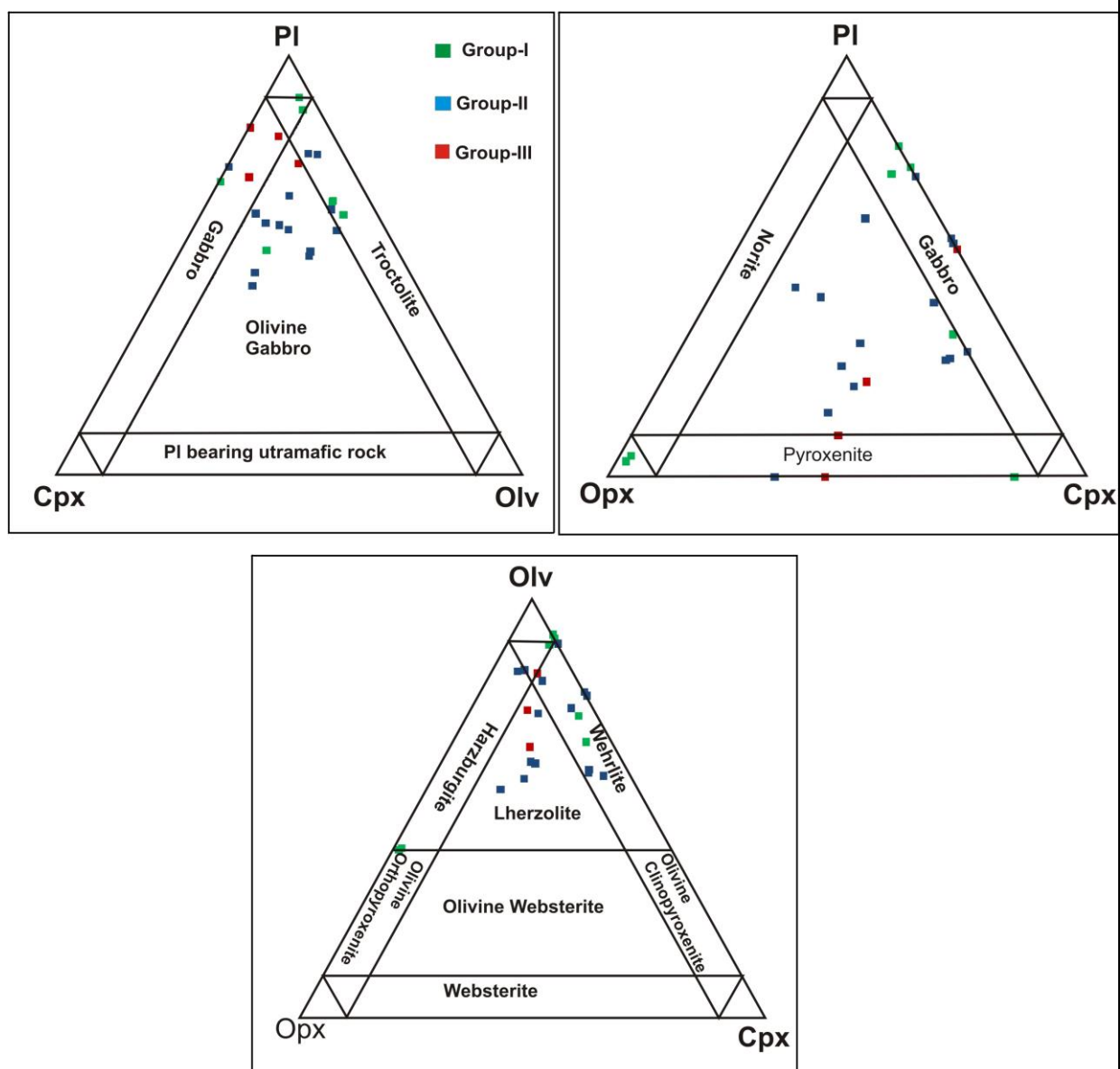
Fig 7. IUGS classification of studied mafic rock

# 5. ELEMENT BEHAVIOUR AND FACTORS CONTROLLING COMPOSITION OF BASIC ROCKS:

Before going to discuss about the geochemistry of the studied dyke,behaviour of different elements should be known.

On the basis on **distribution coefficient** or **partition coefficient** (D=concentration of a trace element in the solid / concentration of Trace element in the liquid) trace elements are two types:

1. Compatible elements:

   Compatible trace elements concentrate in the solid, rather than liquid.

   Here, D>>1

2. Incompatible elements

   Incompatible trace elements are concentrated in the melt more than the solid. Here, D<<1

Incompatible elements are commonly subdivided into two subgroups based on the ratio of valence state to ionic radius.

1. HFSE (high field strength elements)

   They are smaller in size and more highly charged. They include the REE, Th, Ce, $Pb^{4+}$, Zr, Hf, Ti, Nb and Ta.

2. LILE (large ion lithophile elements)

   They are generally considered to be more mobile, particularly if fluid phase is involved. They include K, Rb, Cs, Ba, $Pb^{2+}$, Sr, $Eu^{2+}$.

# Behaviour of elements:

- Ni, Co, Cr- Highly incompatible elements. Ni and Cr are concentrated in Olivine, Cr in spinel and clinopyroxene. High concentrations indicate a mantle source, limited fractionation, or crystal accumulation.

- V, Ti- Both show strong fractionation into Fe-Ti oxides (ilmenite or titano-magnetite). If they behave differently, Ti probably fractionates into an accessory phase, such as sphene or rutile.

- Zr, Hf- Very incompatible elements that do not substitute into major silicate phases (although they may replace Ti in sphene or rutile). High concentrations imply an enriched source or extensive liquid evolution. Negative anomalies indicate predominance of mantle derived sources.

- Ba, Rb- Incompatible elements that substitute for K in micas, K-feldspar or hornblende. Rb substitutes less readily in hornblende than in micas and K-feldspar, so K/Ba ratio may distinguish these phases.

- Sr- Substitutes for Ca in plagioclase (but not in pyroxene), and to a lesser extent, for K in K-feldspar. Behave as compatible elements at low pressure where plagioclase forms early, but as an incompatible element at higher pressure where plagioclase is no longer stable.

- REE- Myriad uses in modelling source characteristics and liquid evolution. Garnet accommodates the HREE more than the LREE and orthopyroxene and hornblende do so to a lesser degree. Sphene and plagioclase accommodates more LREE. $Eu^{2+}$ is strongly partitioned into plagioclase.

- Y- Commonly incompatible. Strongly partitioned into garnet and amphibole. Sphene and apatite also concentrate Y, so the presence of these as accessory phases could have a significant effect.

# Processes controlling element fractionation:

From melt generation and transport from mantle source to crust, magma geochemistry is easily to be changed due to complicated processes, such as fractional crystallization, assimilation, magma mixing, etc. In addition, different degrees of partial melting can also lead to diversity of magmatic compositions.

## Melting:

When a mantle rock begins to melt, the incompatible elements will be ejected preferentially from the solid and enter the liquid. A low degree melting of a mantle rock will have high concentration of incompatible elements. As melting proceeds the concentration of these incompatible elements will decrease because

a) There will be less of them to enter the melt and

b) Their concentration will become more and more diluted as other elements enter the melt. Thus incompatible element concentrations will decrease with increasing % of melting.

Magmas produced by small degree of partial melting

- At shallow depth will be depleted in Sr.

- From intermediate depths will be depleted in V, Cr.

- From depth >80 km will be depleted in HREE.

## Crystallization

Identification of the phases which have fractionated from a magma undergoing fractional crystallization is crucial in understanding the nature and evolution of the magma. The variations in each oxide as a function of decreasing Mg# or MgO result from the crystallization of stable mineral

phases from the melt, which, for typical basaltic melts at, 50–100 MPa pressure, generally includes olivine ± minor spinel, followed by plagioclase and finally clinopyroxene (Kelemen *et al.*, 2003; Klein, 2003). The compositions and proportions of the minerals that crystallize from each melt drive the residual melt to a different (lower MgO) composition. Because these changes represent the changing composition of the melt as it cools, crystallizes, and evolves, the variations are called the "liquid line of descent" for a particular parental (high MgO) magma composition (Kelemen, Hanghoj, & R Greene, 2003; Klein, 2003). Separation of:

a) Plagioclase depletes the remaining melt in Al, Sr and Eu.
b) Olivine depletes it in Mg, Ni, Co.
c) Spinel depletes it in Mg, Fe, V, Cr and possibly Zn.
d) K-feldspar depletes it in Ba and Rb.

For metamorphosed mafic rocks in orogenic belts, the geochemistry that was inherited from the magma can be significantly metasomatized in an early stage of orogenesis, making the geochemistry less diagnostic in distinguishing tectonic settings. In this regard, a combined study on field geology, geochemistry and isotopic geology is necessary to recognize magma sources, petrogenesis and related tectonic settings.

# 6. MAJOR ELEMENT COMPOSITION OF THE ROCK:

**Analytical techniques:** A total of 23 samples were analyzed. Major oxide analyses were carried out in the X-ray Fluorescence laboratory of National Centre for Earth Science Studies (NCESS), India. Major element abundances were analyzed by X-ray fluorescence (XRF) on fused disks using a Bruker S4 Pioneer sequential wavelength-dispersive X-ray spectrometer. Details of the methodology used in these laboratories are discussed in Ravindra Kumar and Sreejith (2016). Standards used for the analyses are G2, GSP2, STM1, SARM1, SARM2, SY3, RGM, GA, GH, GS- N, AC-E, MDOG, ISHG, VS-N, JG-1, JG-2, JG-3, JR-3 and JSY-1.

The studied rocks show the following chemical characters:

- low to moderate $SiO_2$ (38.79-53.55 wt%),
- low to moderate MgO (4.12-11.39 wt%),
- $FeO_{TOTAL}$ (8.42–17.94 wt%),
- CaO (8.00–12.58 wt%),
- High $Al_2O_3$ (12.21–21.95 wt%).
- Moderate $TiO_2$ (0.29-2.76 wt%)
- Negligible $P_2O_5$ (0.03-0.45 wt %)
- The apatite-ilmenite bearing samples have:

   2.63-3.11 wt % $P_2O_5$ and high 3.77-6.10 wt % $TiO_2$.

All samples have moderate total alkalis ($Na_2O + K_2O$ = 0.32-4.15 wt %) but widely variable $Na_2O/K_2O$ ratios (1.33-6.35). The sampled dykes are classified as sub-alkaline basalts on the TAS diagram (Fig.8; Le Maitre et al.,

1989). The boundary line between alkaline and subalkaline series is from Irvine and Baragar (1971).
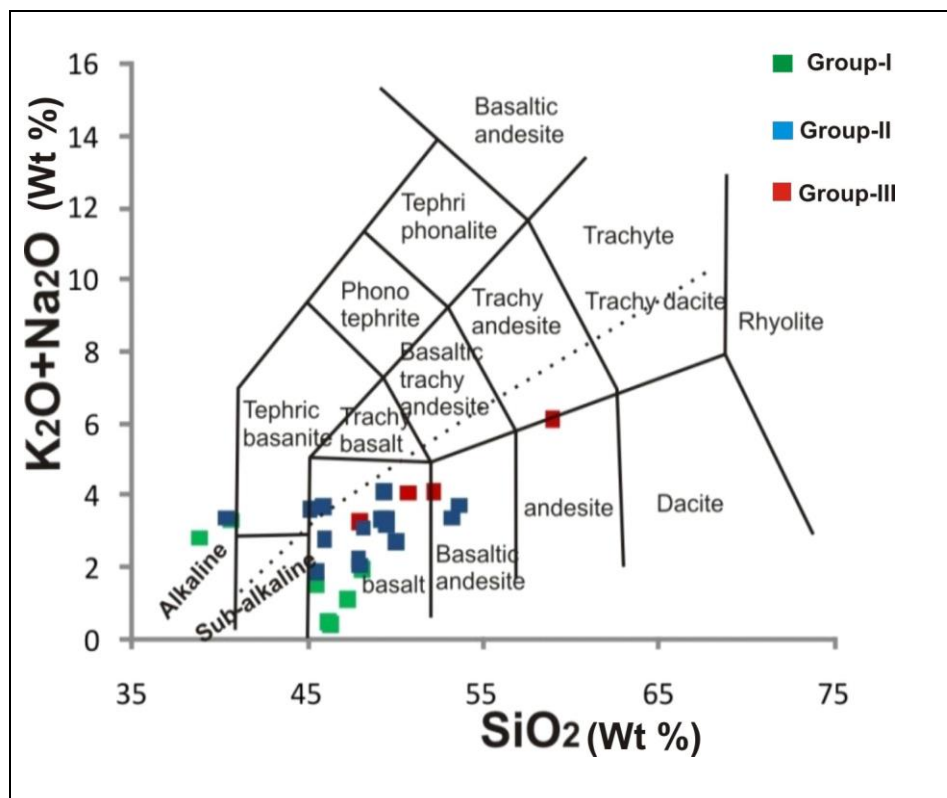


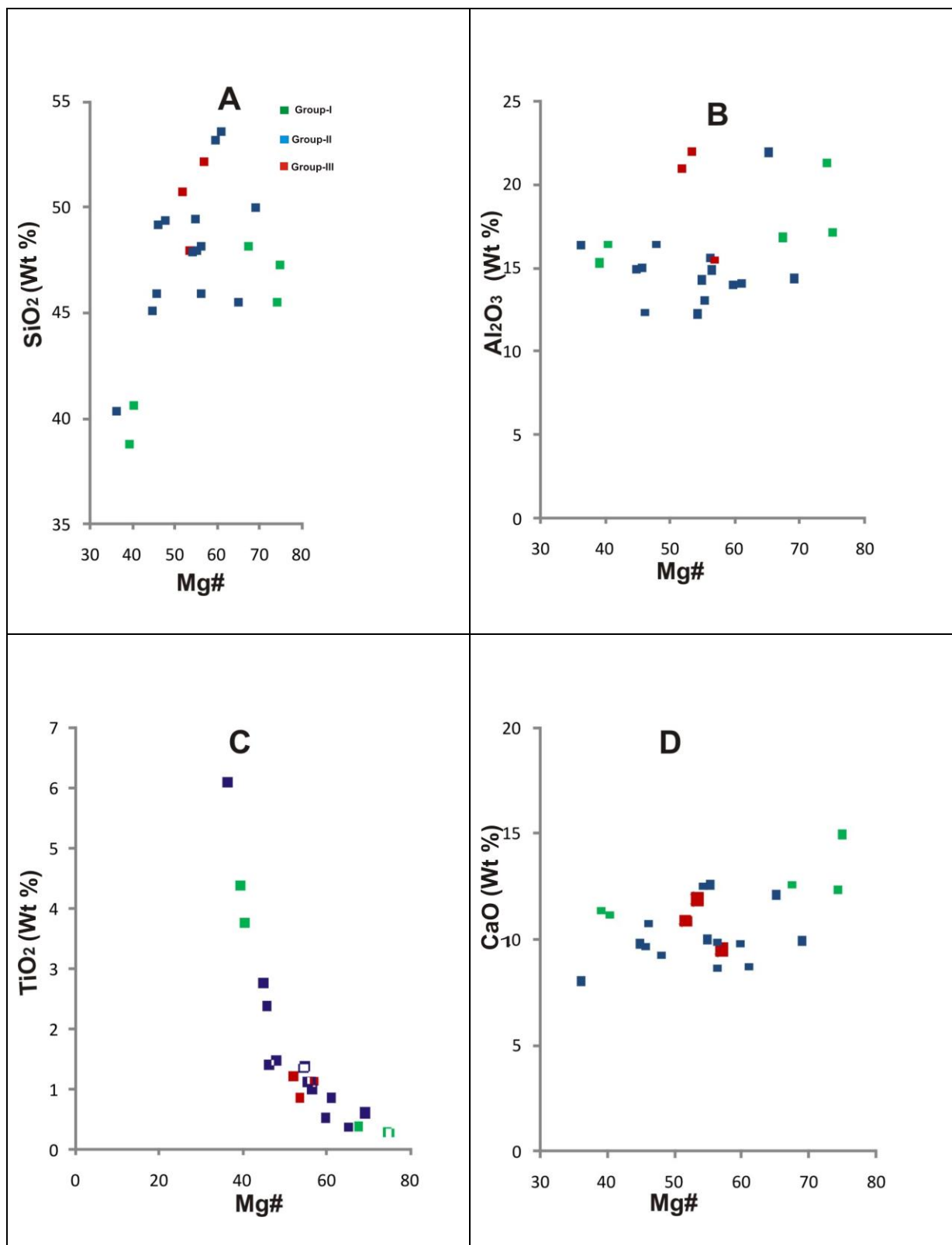**Fig 8. Compositional plots of the studied dykes in the TAS diagram.**

In $K_2O$ vs. $SiO_2$ (Fig.9,Taylor,1969), the samples plot in the field of low to medium K basalt.
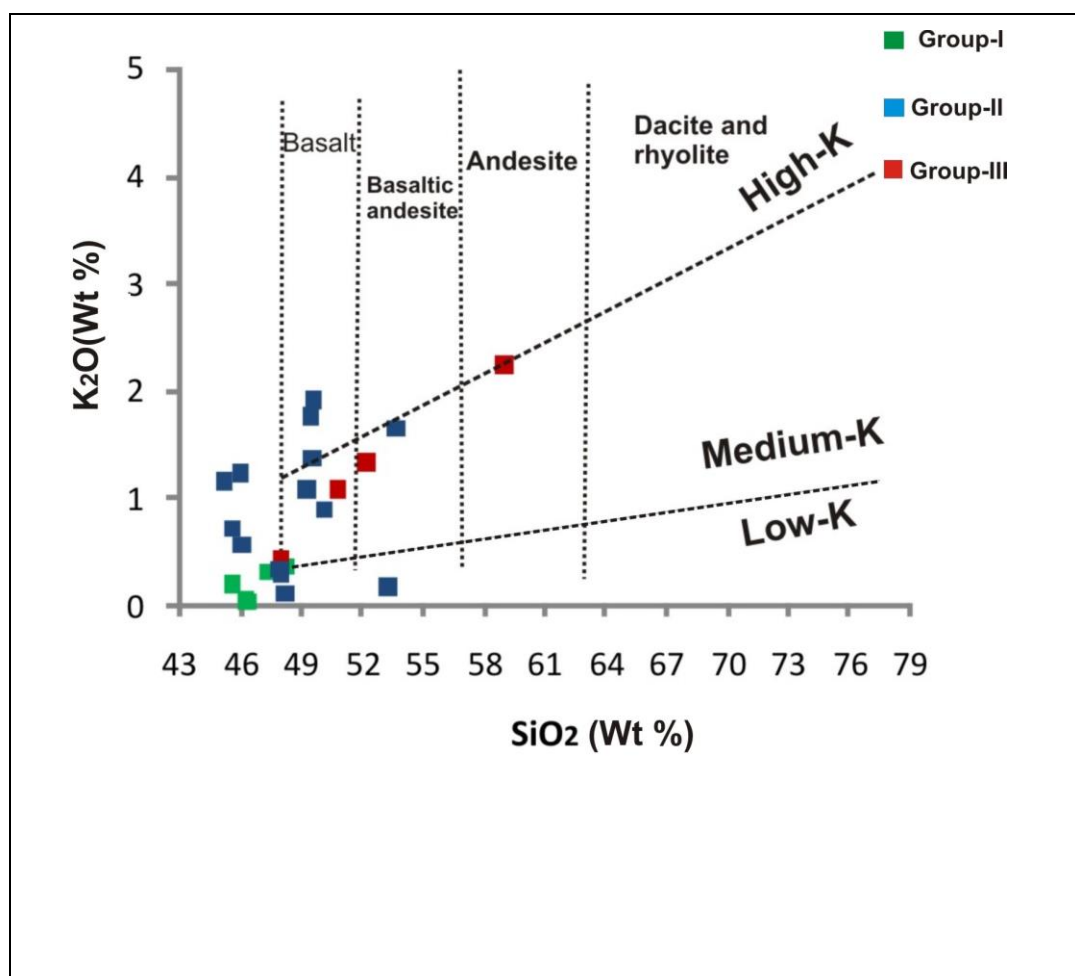
**Fig 9.Compositional plots of the studied dykes in the SiO₂ vs K₂O diagram.**

It has long been known that suites of basic rocks recovered from a relatively limited spatial area often display regular variations in major element oxides as a function of Mg#, defined as [molar 100*MgO/MgO+ FeO$_{TOTAL}$] (Kelemen *et al.*, 2003; Klein, 2003). Mg# of the studied samples varies from 36-69 and the variation of the major oxides have been shown in Fig.10(A) to Fig.10(G), overall Mg# versus SiO₂, TiO₂, FeO$_{TOTAL}$, MgO, CaO and Na₂O for the studied samples closely approximate a single liquid line of descent, and hence appear to result from progressive fractional crystallization:
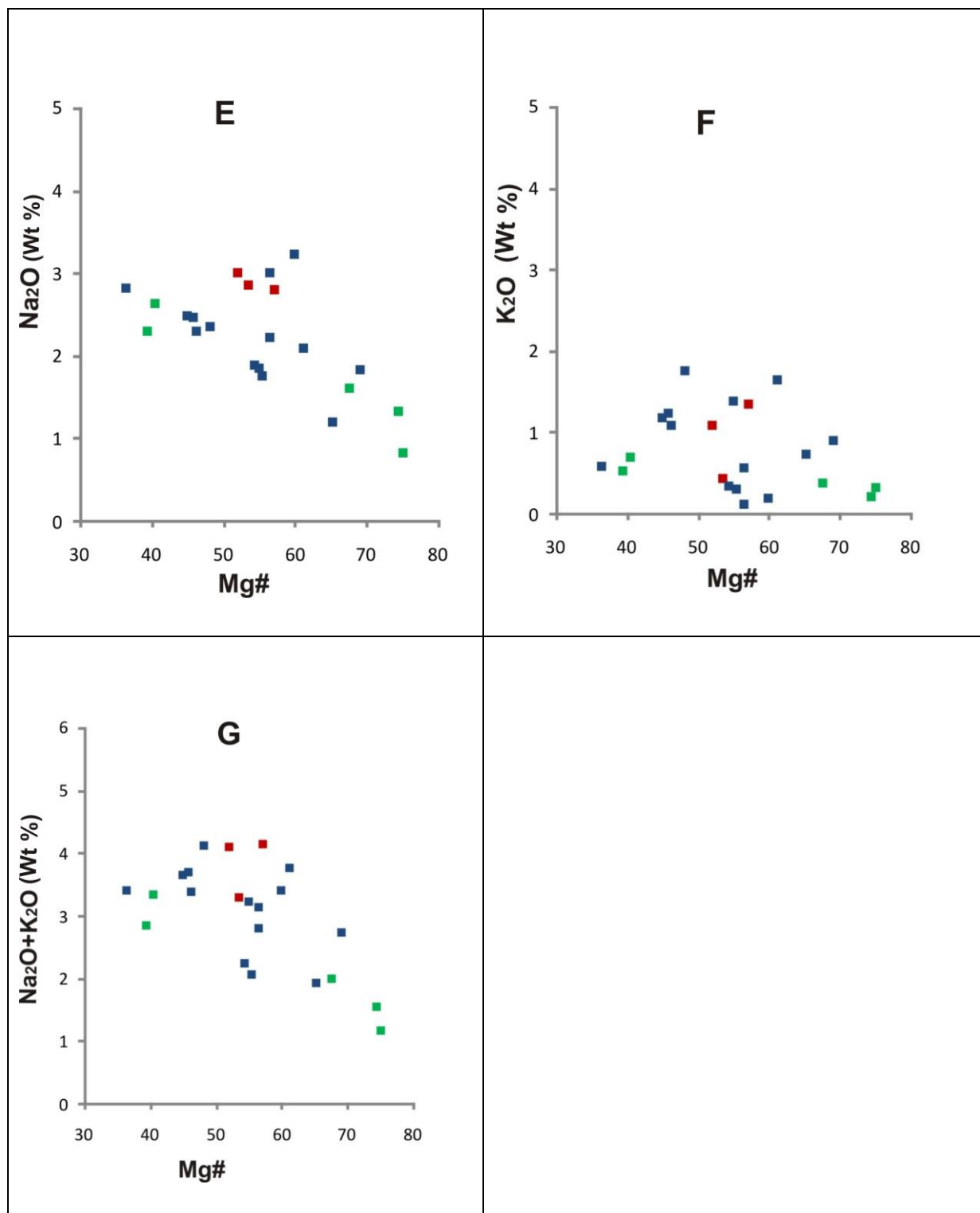
**Fig 10. Compositional plots of the studied dykes in the Mg# vs Different oxide of major elements.**

- Increasing $TiO_2$ with decreasing Mg# ( Fig. 10C) is possibly due to fractionation of Fe-Ti oxides from the evolved melts. The Fe-Ti oxide–apatite–olivine cumulates found in one sample may represent this early fractionated cumulate.

- CaO is not changed with changing of Mg#(Fig. 10D) in melt. It implies the crystallization of some non-ferromagnesian mineral from melt which supports crystallization of plagioclase feldspar from evolved melt. Crystallization of plagioclase feldspar from melt is supported by Mg# vs $Na_2O$ diagram (Fig. 10E) where $Na_2O$ decreases with increasing Mg#.

- Absence of distinct trend in $Al_2O_3$ contents indicates that plagioclase fractionation was probably not that dominant.
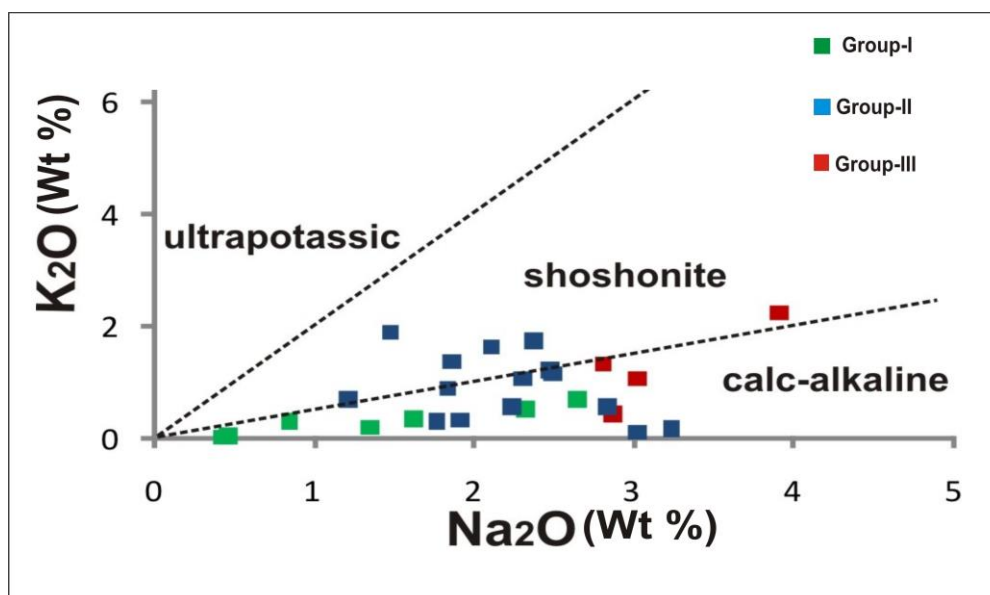


**Fig 11. Compositional plots of the studied dykes in the Na₂O vs K₂O diagram.**

In a plot of K2O vs. Na2O the studied samples plot mainly in the calc-alkaline to shoshonite field (Fig.11).
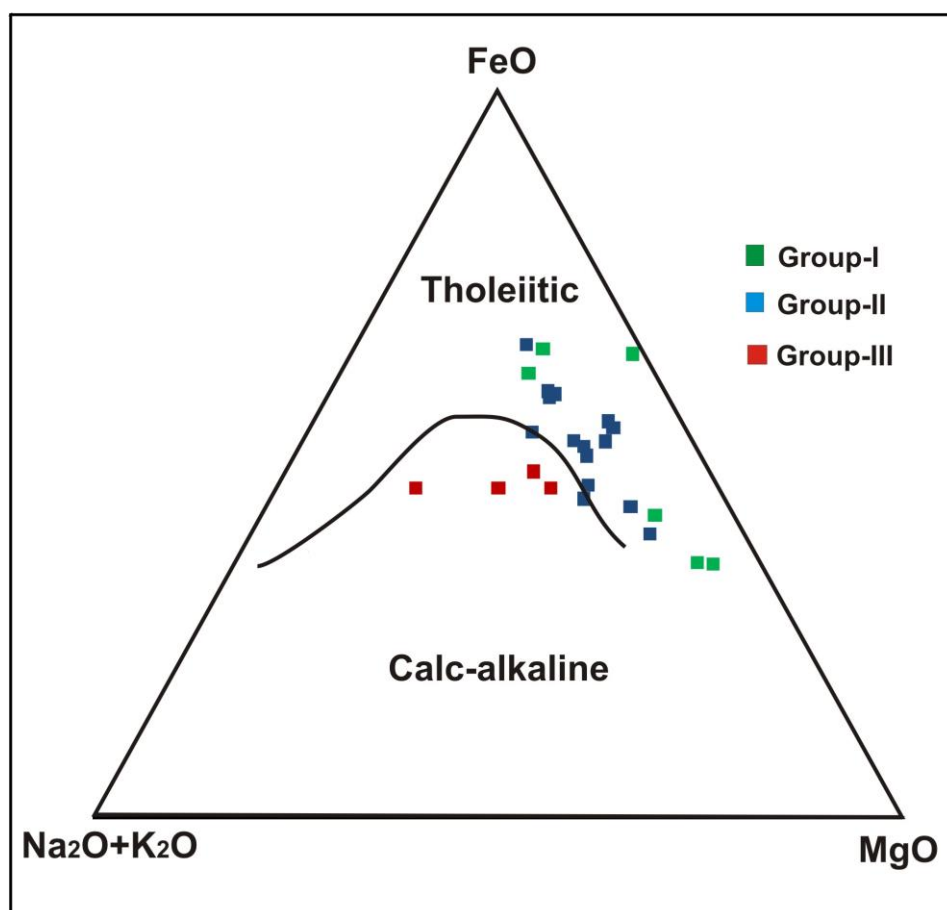


**Fig 12. Compositional variation of the studied dykes in the AFM diagram.**

In a ternary plot of FeO–MgO–[$Na_2O+K_2O$] (AFM) Fig.12. (Irvine and Baragrar,1971), it is seen that some samples lie in Tholeiitic basalt's field and some samples lie in Calc alkaline basalt's field. As described previously, the primary magmatic minerals are variably replaced by secondary minerals (amphibole + biotite). Keeping that in mind, it is seen that the samples of group-III (most altered) plot in the calc-alkaline field. So it can be concluded that the calc-alkaline basalt trend is an artefact of secondary alteration. This is further

supported by decreasing $Na_2O+K_2O$ with increasing Mg# (Fig.10G), as calc-alkaline magmas tend to having both high Na+ K at high Mg#, whereas tholeiitic magmas tend to have lower Na+ K at the same Mg#.

# 7. TRACE AND RARE EARTH ELEMENT COMPOSITION OF THE ROCK:

**Analytical techniques:** Trace element concentration analyses were performed at the Department of Earth Sciences, Indian Institute of Technology Kanpur. Approximately 0.25 g of the provided sample powder was first digested in pre-cleaned Teflon beakers (Savillex) at $130 \pm 5°C$ using a 4 ml mixture of concentrated HF (1 part), concentrated HCl (1 part) and concentrated $HNO_3$ (2 parts) for 48 hours. The acid was then slowly evaporated at $80 \pm 5°C$, and again the samples were re-dissolved in 3 ml of Aqua Regia acid (2 ml of concentrated $HNO_3$ + 1 ml of concentrated HCl). Aqua Regia was fluxed for 24 hours. After Aqua Regia digestion step, the samples were dried and re-dissolved in 2% $HNO_3$. The acid digestion steps were only repeated when digestion was incomplete. For all analytical work, trace element grade pure acid and 18.2 M$\Omega$ cm water from a Millipore water purification system was used. Pure acids were produced by sub-boiling distillation in the Department of Earth Sciences using the Cupola Still system from PicoTrace.

Trace element concentrations were determined at 500 ppm total dissolved solid solutions, whereas for the REEs, it was determined at ~2000 ppm total dissolved solid solutions. Three procedural blanks and Reference Materials BHVO-2 (Basalt) from US Geological Survey (USGS), and WGB-1 (Gabbro) rock standard from Canadian Certified Reference Material Project were also digested following the same procedures. The blanks were analyzed to quantify the total procedural blank, whereas BHVO-2 and WGB-1 were analyzed as an unknown to assess the data quality. A 10 µg/g multi element standard solution from Sigma-Aldrich was diluted to 7 appropriate concentrations to construct the calibration curve (0.1 ng/g, 1 ng/g, 10 ng/g, 20 ng/g, 50 ng/g, 75 ng/g, 100

ng/g), and trace element concentrations were determined against the calibration curve. Since rock-matrix matched reference materials were unavailable, all the samples and standards were spiked by ~5 ppb In solution, which was used as an internal standard. The intensities were corrected for matrix effect using In as an internal standard. Trace elements were determined using an Agilent Triple Quadrupole Inductively Coupled Plasma Mass Spectrometer (QQQ-ICPMS), also known as ICP-MS/MS. The instrument was run both with no gas and with reaction gases namely oxygen and helium to optimize the separation of measured isotopes from interfering polyatomic interferences. Few samples were run in duplicates to check the reproducibility of the numbers, and they were well reproduced. The final concentrations were blank – corrected using the average procedural blank concentrations and matrix effect was corrected by In normalization. Average blank corrections were less than 1% for most of the elements. All the 29 elements agreed well with their certified values.

The chondrite normalized rare earth element patterns of the studied samples (Fig.13(A)) show:

- moderate enrichment of light REE (LREE) with average $La_{CN}/Yb_{CN}$ = 5.54 and $La_{CN}/Sm_{CN}$ = 2.43; CN refers to the respective chondrite-normalized values.
- the heavy REE (HREE) profiles are nearly flat, with low $Tb_{CN}/Yb_{CN}$ = 1.24), slightly higher than the average value of E-MORB (~1.11).

The primitive mantle-normalised trace element patterns show:

- depletion of high field strength elements (HFSE) with prominent negative anomalies of Nb, Zr and slight negative anomaly of Ti (Fig.13(B));
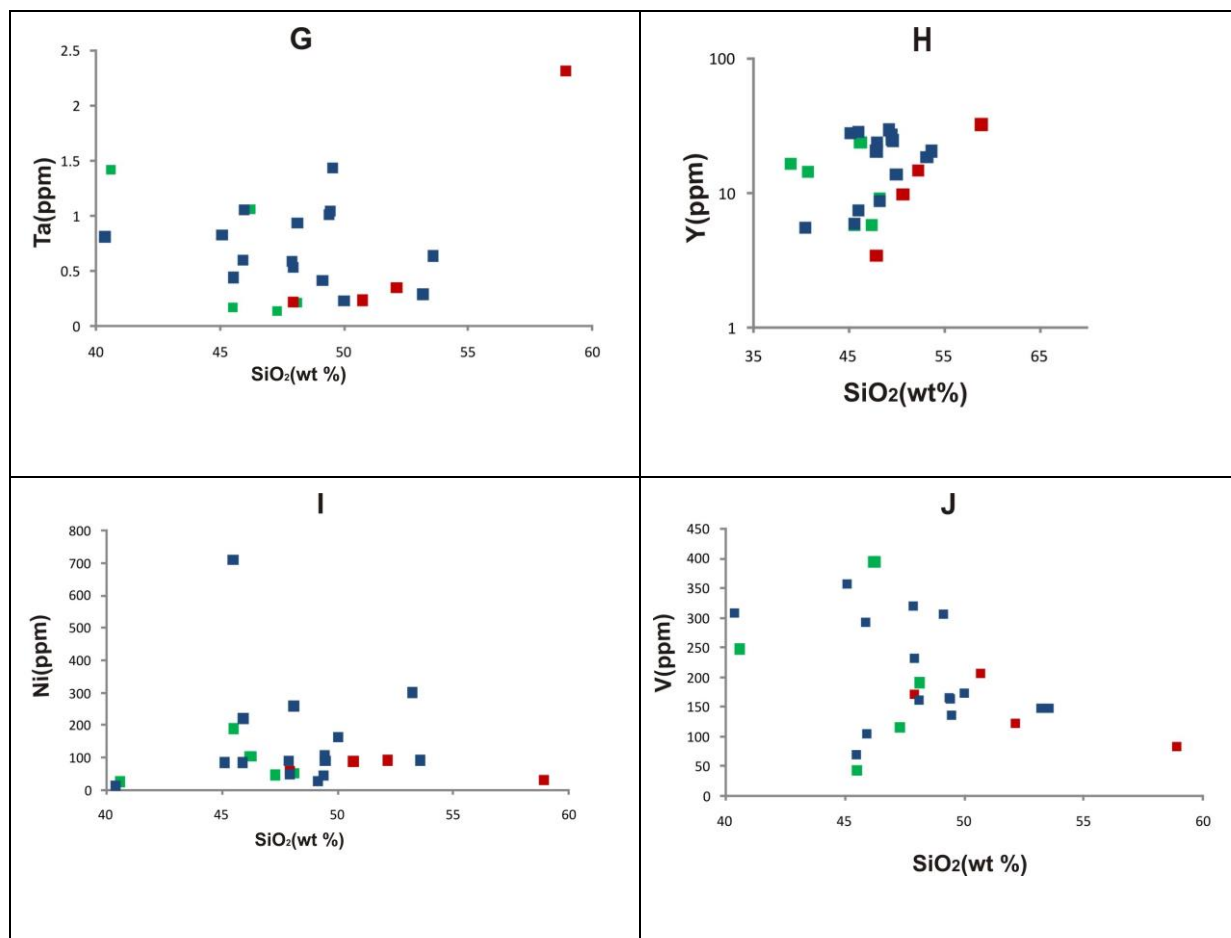- enrichment in Rb.
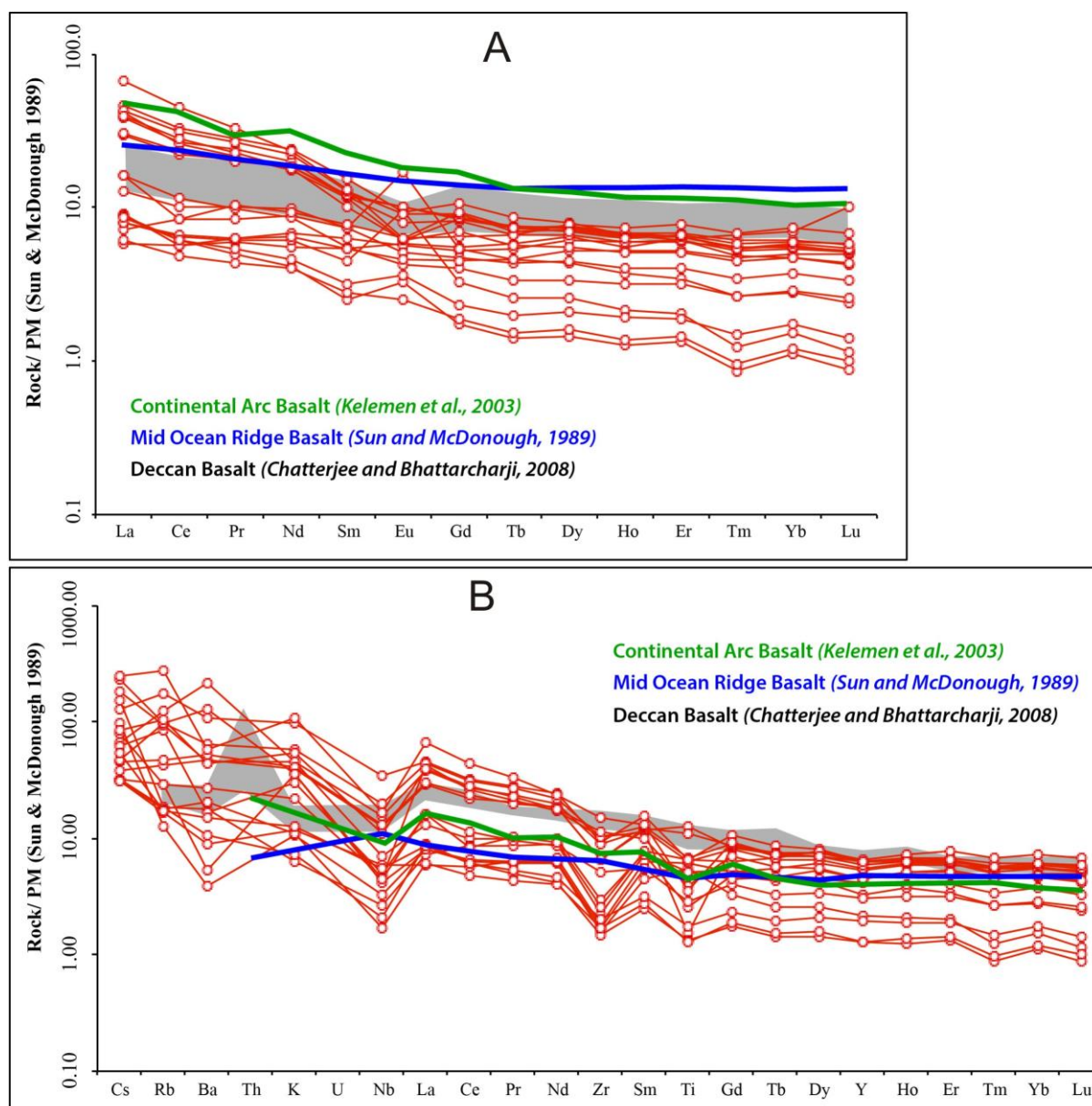
**Fig 13.(A) Spider diagram  (B).Trace element pattern of studied mafic dyke**

These patterns are very similar to the patterns shown by the average values of continental arc basalts as compiled by Kelemen et al. (2003) and Deccan basalts (continental flood basalts) from Chatterjee and Bhattarji (2008) (Fig. 13(A-B)).
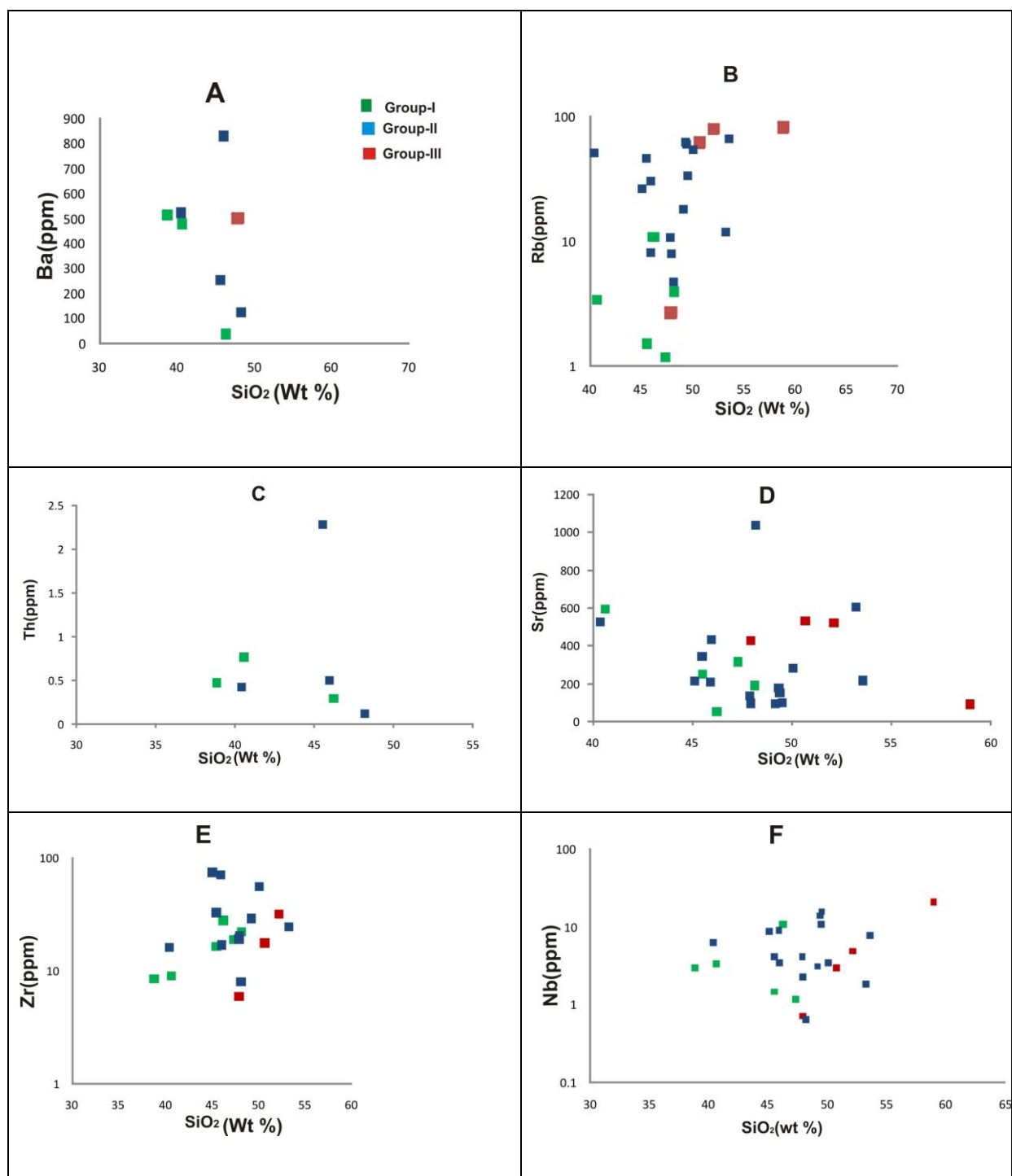
**Fig 14. Compositional plots of studied dyke in the SiO2 vs different trace element diagrams**

In plots of $SiO_2$ vs. trace elements like Ba, Rb, Sr, Th, Zr, Nb, Ta, Y, Ni and V diagram (Fig.14), there is no particular trend.They remain in scattered form.

# 8. GEOCHEMICAL CRITERIA FOR DISCRIMINATION BETWEEN TECTONIC SETTING:

Discriminant analysis is a statistical technique used for classifying sample into predefined groups. A large number of variables are examined in order to isolate the ones which most effectively classify the samples. The most powerful discriminants are used to define the axes on bivarient and triangular diagrams. The separate groups of samples are plotted either as elemental concentrations or as calculated discriminant functions based upon the elemental concentration, and boundaries are drawn between the different groups of samples. Unkown samples are then classified according to the defined fields. In the case of the study by Pearce and Cann (1971, 1973) the elements Ti, Zr, Y, Nb and Sr were found to be the most effective discriminants between basalts erupted in different tectonic environments.

The number of tectonic environments, in which magmas may be generated, recognized today is much greater than 20 years ago. This reflects the advances made in understanding both earth processes and the chemistry of Igneous rocks. The different tectonic settings for basic rocks (Rollinson, 1993) are:

## 1. <u>WBP (within-plate basalts):</u>

Within plate basalt (WPB) is generated within a continental or oceanic plate, rather than at active (constructive or destructive) plate margin. Continental floodbasalt and ocean island basalt are types of within plate basalts. WPB basalt mainly contains (Rollinson, 1993)

- ○ High Ti,Zr
- ○ Low Y
- ○ High Zr/Y,Ti/Y
- ○ High Nb/Y
- ○ Higher Ce/Sr ratio than volcanic arc basalt
- ○ Low $K_2O$/Yb
- ○ High range of Cr

## 2. <u>IAT (island- arc tholeiites):</u>

Island arc tholeiites is a part of volcanic arc basalt. It is formed when an oceanic plate is subducted under on other oceanic plate. Tholeiitic basalt within island arc is related to shallow depth. IAT consists of (Rollinson, 1993)

- ○ Low Ti, Zr, Nb, Y
- ○ High Sr
- ○ Hf/Th > 3
- ○ Zr/Y < 3
- ○ 10 < Ti/V < 20
- ○ Low LREE and HFS elements
- ○ Wide range of Cr
- ○ Lower Ce/Sr than MORB
- ○ High $K_2O$/Yb
- ○ $K_2O$/$H_2O$ > 0.7
- ○ Low in Fe  content

# 3. <u>IAB (island-arc basalts):</u>

IAB is related to subduction zone. It is associated with volcanic arc. There are generally 3 type of volcanic series from which the types of volcanic rock that occur in island arcs are formed

   a)  Tholeiitic series

   b)  Calc-alkaline series

   c)  Alkaline series.

Geochemical signatures of tholeiitic basalts (Rollinson, 1993):

     o     Low Ti, Zr

     o     Lower  Cr than MORB

     o     Wide range of MORB.

     o     Lower Ce/Sr than MORB & WPB

     o     High $K_2O/Yb$

     o     $K_2O/H_2O > 0.7$

Geochemical signatures of tholeiitic basalts:

Calc alakaline basalt is generated from greater depth compare to tholeiitic basalt (Rollinson, 1993):

     o     Low Ti

     o     High Zr, Y, Sr

     o     Hf/Th < 3

     o     15 < Ti/V < 50

     o     High Th, Ce, P, Sm.

     o     Ce/Sr is less than MORB

     o     High $K_2O/Yb$

     o     $K_2O/H_2O > 0.7$

     o     Wide range of Cr

## 4. MORB (mid-ocean ridge basalts):

MORB is generated in divergent plate boundary. Here, tholeiitic basalt is mainly formed and it originates from much closer to earth's surface in the asthenosphere. MORB is of 2 type.

a) N-MORB(normal MORB)
b) E-MORB or P-MORB(enriched MORRB or Primitive MORB)

Geochemical signatures of MORB are mainly (Rollinson, 1993):

- o  Low Ti/Y
- o  Low Nb/Y
- o  High Y
- o  $50 < Ti/V < 100$
- o  High Cr
- o  $K_2O/H_2O < 0.7$
- o  Higher Ce/Sr than Volcanic arc basalt
- o  $Zr/Nb > 30$ (for N-MORB)

## 5. OIT (ocean island tholeiite):

OIT is one type of OIB (ocean island basalt) which dominant by tholeiitic series. It is associated with mantle plume and hotspots. Here crustal contamination is minimum. Geochemical signatures of OIT (Rollinson, 1993):

- o  Low $P_2O_5$
- o  Low $TiO_2$
- o  $K_2O/H_2O > 0.7$
- o  $12\% < CaO + MgO < 20\%$
- o  Richer in LREE than MORB
- o  $20 < K/Ba < 40$
- o  $Zr/Nb < 20$

- o La/Yb = 4

# 6. OIA (ocean island alkaline basalt):

OIT is one type of OIB (ocean island basalt) which dominant by alkaline series. OIA is associated with Mantle plume & hotspots. Here, crustal contamination is also minimum. Geochemical signatures of OIA (Rollinson, 1993):

- o Low Y/Nb
- o Higher LREE and HFS elements than OIT
- o K/Ba > 20
- o Zr/Nb < 20
- o La/Yb = 12
- o $K_2O/H_2O > 0.7$

# 9. TECTONIC CLASSIFICATION OF STUDIED MAFIC DYKES:

The compositions of the studied samples were plotted in the following tectonic classification diagrams:

Fig.15(A).    **TiO$_2$-MnO-P$_2$O$_5$** discrimination diagram for basalt
(Mullen,1983).

Fig.15(B): **Ti-Zr-Y** discrimination diagram for basalt (Pearce & Cann, 1973).

Fig. 15(C): **Ti-Zr-Sr** discrimination diagram for basalt (Pearce & Cann 1973).
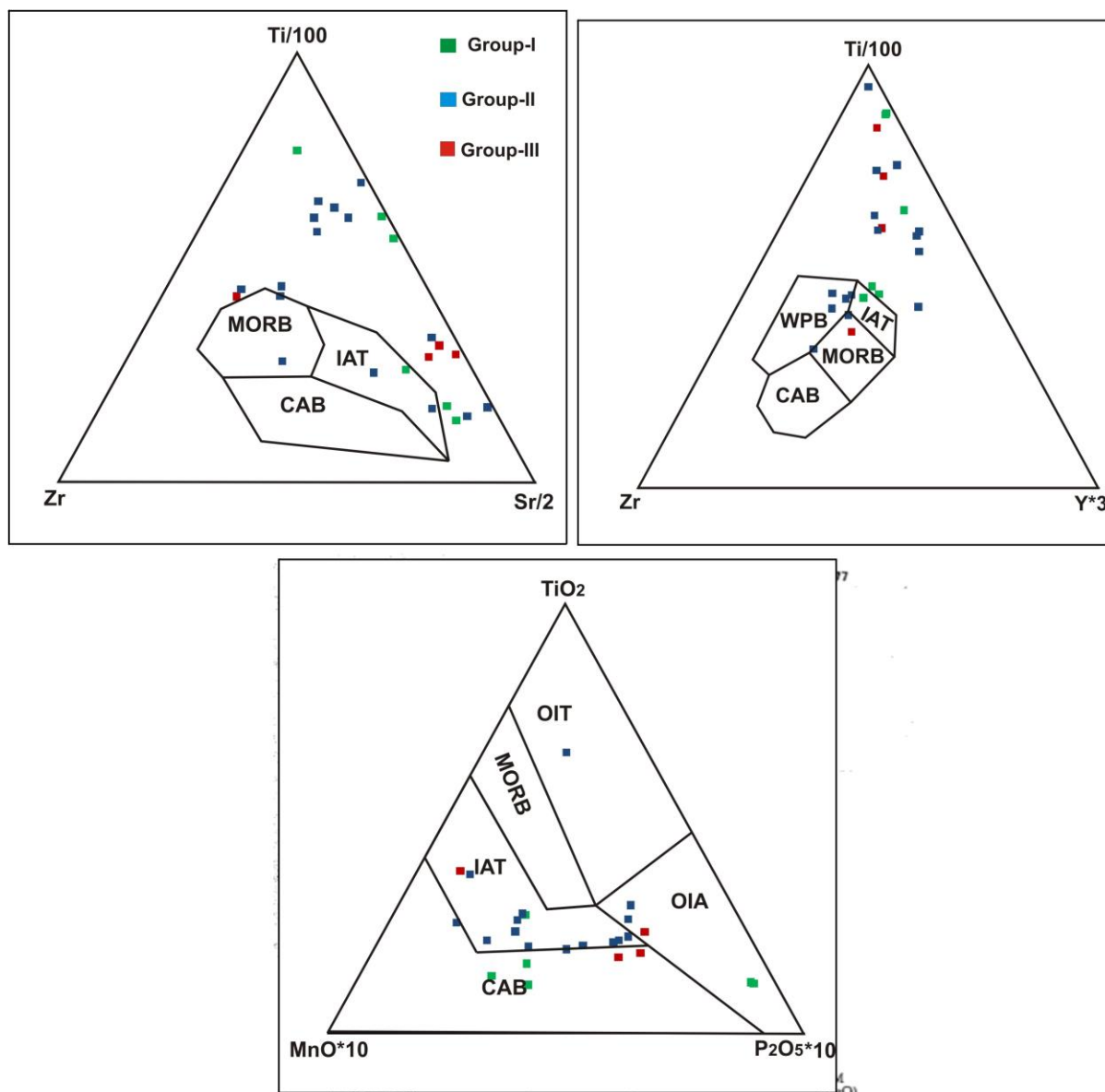
**Fig 15. Compositional variations in studied mafic dyke in the Tectonic discrimination diagrams for basalt.**

It is shown in the above diagrams that rock samples remain scattered and do not define any clusters whatsoever. Sometimes, some samples are plotted in the field of IAT (Island arc tholeiite), whereas other samples are plotted in WPB (within plate basalt) field. So, from the above diagrams, we can't interpret the exact tectonic setting in which this rock was generated. As has been stated previously, discriminant analysis is a statistical technique used for classifying

sample into predefined groups. This implies that there are or should be some statistical parameters/limitations of using such diagrams. From the present study, it can be concluded that these tectonic discrimination diagrams are not applicable in the following cases:

- ➢ Tectonic discrimination diagrams are applicable for a particular concentration of Ti (Ti < 5000 ppm, Rollinson,1993). In our rock samples, concentration of Ti is comparatively higher than the amount of Ti which is required for these tectonic discrimination diagram. But, there is no particular range of higher and lower value of Ti range for which this discrimination diagram is applicable.

- ➢ Concentration of Zr and Y in the studied samples is also lower than the range for which the diagrams can be used (25< Zr < 100 ppm & 4<Y<14, Rollinson, 1993).But there is no particular range of concentration of trace elements for which these discrimination diagram is applicable.

Many workers use these diagrams for low-moderate grade metamorphosed rocks stating that since melting did not occur in those rocks, significant element exchange did not occur. In this study the samples do not yield proper constrain for interpreting the tectonic settings. Therefore, these diagrams should be used with caution and with proper support from other geological observations.

# 10. DISCUSSION:

As some unaltered samples preserve the ophitic texture (Fig. 4B), it can be interpreted that our studied rock was formed due to rapid cooling at shallow crustal depth at least 3-5 Km from surface (Winter, 2001). As some rock samples consists of large phenocryst of apatite, olivine & clinopyroxene (Fig. 5C), It can be said that these phenocrysts are formed at higher depth and is carried with magma to shallower depth. The geochemical characters of the most of the mafic dykes are plotted in the field of tholeiitic basalt (Fig. 12) . Some rock samples are plotted in calc-alkaline field, but this enrichment of alkali elements Na+ K seems to be the artefact of alteration during metamorphism of the dykes. This basalt is slightly enriched in LREE and resembles the composition of continental arc or flood basalts. In compositional variation of mafic dyke in the $SiO_2$ vs. different trace elements diagrams (Fig. 14), absence of any particular trend and their scattered form suggests that it arises due to metasomatism. Nb troughs evident in the samples (Fig. 13B) suggest the contribution of metasomatized lithospheric mantle in their mantle sources. However, the moderate to high $TiO_2$ contents cannot be explained by melting of the metasomatized lithospheric mantle. Thus it is likely that the source magmas were produced through a lower degree of partial melting of deep asthenospheric mantle. The strong Zr depletion supports the deep asthenospheric mantle source. The magmas from asthenosphere may interact with the melts from metasomatized lithospheric mantle to form the Nb depletions. By applying tectonic discrimination diagram, the samples do not yield proper constrain for interpreting the tectonic settings. So, these discrimination diagrams can not be used in every cases for interpreting the tectonic settings. Therefore, these diagrams should be used with caution and with proper support from other geological observation.

# REFERENCES:

A. Roy, M. H. Prasad and S.K. Bhowmik (2001)- Recognition of Pre-Grenvillian and Grenvillian Tectonothermal Events in the Central Indian Tectonic Zones: Implications on Rodinian Crustal Assembly.

A. Roy, M. H. Prasad (2002)- Tectonothermal events in Central Indian Tectonic Zone (CITZ) and its implications in Rodinian crustal assembly.

G. L. Farmer (2003)-Continental Basaltic Rocks. In: *Treatise on Geochemistry*. Elsevier, 1–39.

F. Gallien, A. Mogessie, C. A. Hauzenberger, E. Bjerg, S. Delpino and B. Castro de machuca (2012)- On the origin of multi-layer coronas between olivine and plagioclase at the gabbro–granulite transition, Valle Fertil–La Huerta Ranges, San Juan Province, Argentina.

Geert-Jan L.M. de Haas, T. G. Nijland, P. J. Valbracht , C. Maijer, R. Verschure , T. Andersen (2002)- Magmatic versus metamorphic origin of olivine-plagioclase coronas.

H. M. Lang, A. J.Wachter, V. L. Peterson & J. G. Ryan (2004)- Coexisting clinopyroxene/spinel and amphibole/spinel symplectites in metatroctolites in from the Buck Creek uitramafic body, North Carolina Blue Ridge.

H. R. Rollinson (1993) -Using geochemical data-Evalution,presentation & Interpretation.

J. R. Ashworth and V. S. Sheplev (1997)- Diffusion modelling of metamorphic layered coronas with stability criterion and consideration of affinity.

P. B. Kelemen, K. Hanghoj & A. R. Greene, (2003)-One view of the

geochemistry of subduction-related magmatic arcs, with an emphasis on primitive andesite and lower crust. In: *Treatise on Geochemistry*. Elsevier, 593–659.

E. M. Klein  (2003)- Geochemistry of the Igneous Oceanic Crust. In: *Treatise on Geochemistry*. Elsevier, 433–463.

L. Nicholas, T. Arndt, Q. Tang, E. M. Ripley (2015)-Trace element indiscrimination diagrams.

L. Xia, L. Xiangmin  (2018)-Basalt geochemistry as a diagnostic indicator of tectonic setting.

S. Mukherjee, A. Dey, S. Sanyal & P. Sengupta  (2018)- Tectonothermal imprints in a suite of mafic dykes from the Chotanagpur Granite Gneissic complex (CGGC), Jharkhand, India: Evidence for late Tonian reworking of an early Tonian continental crust. *Lithos*, *320-321*, 1–25.
http://doi.org/10.1016/j.lithos.2018.09.014

R. Joesten (1986)-The role of magmatic reaction, diffusion and annealing in the evolution of coronitic microstructure in troctolitic gabbro from Ris6r, Norway.

S. K. Bhowmik (2019)- The current status of orogenesis in the Central Indian Tectonic  Zone: A view from its Southern Margin.

S. K. Acharyya (2002)- The Nature of Mesoproterozoic Central Indian Tectonic Zone with Exhumed and Reworked Older Granulites.

S. S. Sun & W.F. McDonough (1989)- Chemical and isotopic systematics of oceanic basalts: implications for mantle composition and processes.

S. Eggins (1989)- The Origin of Primitive Ocean Island and Island Arc Basalts.

Z. J. bai, H. Zhong, C. Li, W. G. Zhu, & W. J. hu (2016)-Association of cumulus apatite with compositionally unusual olivine and plagioclase in the Taiha Fe-Ti oxide ore bearing layered mafic-ultramafic intrusion: Petrogenetic significance and implications for ore genesis.

# ACKNOWLEDGEMENT

Swagata Maity

Swagata Maity                                                         Date: 31/05/2019
Department of Geological Sciences
Jadavpur University , Kolkata-32